Journal of Sound and Vibration 330 (2011) 127–135

Contents lists available at ScienceDirect

Journal of Sound and Vibration

journal homepage: www.elsevier.com/locate/jsvi

The influence of mass imperfections on the evolution of standing waves in slowly rotating spherical bodies

Michael Y. Shatalov [a,b], Stephan V. Joubert [a,*], Charlotta E. Coetzee [a]

[a] Department of Mathematics and Statistics, Tshwane University of Technology, P.O. Box X680, Pretoria 0001, South Africa
[b] CSIR, Material Science and Manufacturing, Sensor Science and Technology, P.O. Box 395, Pretoria 0001, South Africa

ARTICLE INFO

Article history:
Received 25 June 2009
Received in revised form
22 June 2010
Accepted 2 August 2010
Handling Editor: M.P. Cartmell
Available online 23 August 2010

ABSTRACT

Standing waves can exist as stable vibrating patterns in perfect structures such as spherical bodies, and inertial rotation of the body causes precession (Bryan's effect). However, an imperfection such as light mass anisotropy destroys the standing waves. In this paper, an imperfection is introduced in the form of light mass anisotropy for a vibrating, slowly rotating spherical body. Assuming this light mass imperfection throughout this paper, the effects of slow rotation and light isotropic viscous damping are considered in a system of variables consisting of the amplitudes of principal and quadrature vibrating patterns, the angle of the rotation of the vibrating pattern (called the *precession angle*) and the phase shift of the vibrating pattern. We demonstrate how a combination of both qualitative and quantitative analysis (using, inter alia, the method of averaging) predicts that the inertial angular rate does not influence changes with time in the amplitudes of the principal and quadrature vibrations or the phase shift. The light mass imperfection causes changes with time which appear to be of a damped oscillatory nature for both the quadrature component as well as the principal component. The precession angular rate appears to depend on the inertial angular rate as well as the quadrature component of the vibration but is not influenced by the damping factor. It is not directly proportional to the inertial angular rate as is the case for a perfect isotropically damped structure. If the quadrature component is not suppressed, then a "capture effect" appears to occur, namely that the precession angle will not grow at a constant rate but is "captured" and shows periodic behaviour. It is evident that the damping factor does not influence changes with time in the phase shift and that the mass imperfection substantially influences these changes. The phase shift appears to be negative, strictly decreasing and unbounded.

1. Introduction

In symmetrically distributed structures subjected to vibration and an inertial rotation, the vibrating pattern rotates at a rate proportional to the inertial angular rate. This effect, known as "Bryan's effect" in the sequel, was first observed by Bryan in 1890 [1]. The coefficient of proportionality between the inertial and vibrating pattern rates is known as Bryan's factor. In a recent article, Shatalov et al. [2] confirmed the observation of Zhuravlev and Klimov [3] that Bryan's factor depends on the vibration mode. In addition, they demonstrated that Bryan's factor depends on properties such as Young's

* Corresponding author. Tel.: +27 123826358; fax: +27 123826114.
E-mail address: joubertsv@tut.ac.za (S.V. Joubert).

0022-460X/$ - see front matter © 2010 Elsevier Ltd. All rights reserved.
doi:10.1016/j.jsv.2010.08.001

modulus and Poisson's ratio and they pointed out that it depends on the geometry of the vibrating body. It was further demonstrated that the introduction of light isotropic (viscous) damping does not affect Bryan's effect or Bryan's factor.

In reality, imperfections cannot be ignored in the manufacture of resonator gyroscopes (see Loper and Lynch [4]) because such imperfections cause departures from ideal mass, stiffness and damping distributions and therefore affect resonator dynamics. In this study, by means of a linear theory of elasticity, we introduce light mass imperfections and light isotropic damping into the equations of motion. In so doing, we develop mathematical tools which will facilitate future study which we have earmarked to include nonlinear elasticity, prestress and anisotropic damping.

Standing waves can exist as stable vibrating patterns in perfect structures, such as spherical bodies, but mass anisotropy destroys the standing waves. The equations of motion introduced in [2] are reformulated with light mass imperfection and light isotropic damping taken into account. The two degrees of freedom (and their time derivatives) considered in [2] are transformed into four new variables. These new variables consist of the amplitudes of the principal and quadrature vibrating patterns, the angle of the rotation of the vibrating pattern (called the *precession angle*) and the phase shift of the vibrating pattern. The solutions obtained for the "new" equations of motion are analysed by means of the method of averaging (see Lynch [5]) and visualised by means of computer algebra. We demonstrate how a combination of both qualitative and quantitative analysis predicts that the inertial angular rate does not influence changes with time in the amplitudes of the principal and quadrature vibrations or the phase shift. The light mass imperfection causes changes with time which appear to be of a damped oscillatory nature for both the quadrature component as well as the principal component. The precession angular rate appears to depend on the inertial angular rate as well as the quadrature component of the vibration but is not influenced by the damping factor. It is not directly proportional to the inertial angular rate as is the case for a perfect isotropically damped structure. If the quadrature component is not suppressed, then a "capture effect" appears to occur, namely that the precession angle will not grow at a constant rate but shows periodic behaviour. It is evident that the damping factor does not influence changes with time in the phase shift and that the mass imperfection substantially influences these changes. The phase shift appears to be negative, strictly decreasing and unbounded.

We repeat the notation of [2] with a small modification as depicted in Fig. 1. Indeed, consider a coordinate system $Oxyz$ and a spherical body, with its centre at the origin O. We convert to spherical coordinates $Or\theta\phi$ as depicted in Fig. 1. Consider the position of rest $P(r,\theta,\phi)$ of a vibrating particle in the sphere. Let $\hat{\mathbf{r}}$ be the unit vector in the direction of increasing r. Hence the position vector of the point $P(r,\theta,\phi)$ is $\mathbf{r}=r\hat{\mathbf{r}}$. Consider the usual unit vectors $\hat{\boldsymbol{\phi}}=\partial\mathbf{r}/\partial\phi/|\partial\mathbf{r}/\partial\phi|$ (in the direction of increasing ϕ) and $\hat{\boldsymbol{\theta}}=\partial\mathbf{r}/\partial\theta/|\partial\mathbf{r}/\partial\theta|$ (in the direction of increasing θ). Let $\mathbf{w}+\mathbf{u}+\mathbf{v}$ (where $\mathbf{w}=w\hat{\mathbf{r}}$, $\mathbf{u}=u\hat{\boldsymbol{\theta}}$ and $\mathbf{v}=v\hat{\boldsymbol{\phi}}$) represent the displacement from the position of rest of the vibrating particle (see Fig. 1). The position vector of the vibrating particle is thus

$$\mathbf{R}=(r+w)\hat{\mathbf{r}}+u\hat{\boldsymbol{\theta}}+v\hat{\boldsymbol{\phi}}. \tag{1}$$

Now consider an inertial coordinate system $OXYZ$ with origin O where initially the X, Y, Z-axes correspond to the x, y, z-axes, respectively. Let the spherical body (the $Or\theta\phi\equiv Oxyz$ system) rotate about the z-axis with a small constant angular rate $\varepsilon\Omega$ with respect to inertial space $OXYZ$ (here ε is a "small" parameter, characterizing smallness of the angular rate when compared to the lowest eigenvalue of the vibrating sphere). Consequently, we will neglect centrifugal effects and all terms of $O(\varepsilon^2)$. If $\hat{\mathbf{k}}$ is the unit vector in the direction of increasing z, then the angular velocity $\boldsymbol{\Omega}$ of the body is

$$\boldsymbol{\Omega}=\varepsilon\Omega\hat{\mathbf{k}}=\varepsilon\Omega(\hat{\mathbf{r}}\cos\theta-\hat{\boldsymbol{\theta}}\sin\theta). \tag{2}$$

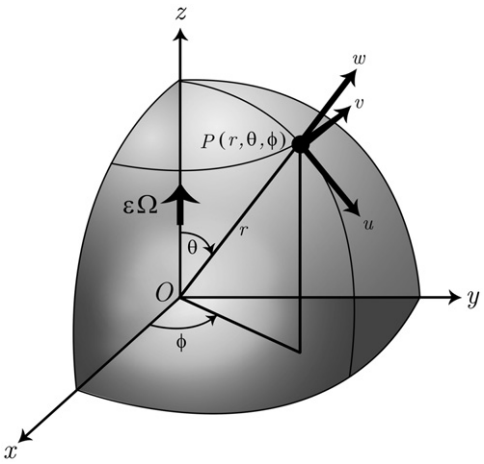

Fig. 1. The spherical coordinate system.

2. Gyroscopic effects for a sphere with light mass imperfections

In this study, we assume that there is a small variation in the density of the spherical body under consideration. The inclusion of anisotropic damping, prestress, nonlinear elasticity and methods to control their effects in a gyroscope is beyond the scope of this paper and has been earmarked for future study.

For the sake of simplicity, assume that the density of the spherical body, ρ, depends only on the circumferential angle, ϕ. This simplification illustrates all phenomena which need to be observed for light mass imperfections. Consequently, assume that $\rho=\rho(\phi)$ with the Fourier expansion

$$\rho(\phi)=\rho_0\left(1+\varepsilon\sum_{k=1}^{\infty}(a_k\cos k\phi+b_k\sin k\phi)\right), \tag{3}$$

where ε is the small positive quantity mentioned above and, in this instance, is a measure of the small variation of density with circumferential angle ϕ. One assumes, as in [2], that a solution to the equations of motion of the m, n-vibration mode may be expressed by

$$\begin{aligned} u_{m,n}(r,\theta,\phi,t)&=U(r,\theta)[C(t)\cos m\phi+S(t)\sin m\phi],\\ v_{m,n}(r,\theta,\phi,t)&=V(r,\theta)[C(t)\sin m\phi-S(t)\cos m\phi],\\ w_{m,n}(r,\theta,\phi,t)&=W(r,\theta)[C(t)\cos m\phi+S(t)\sin m\phi], \end{aligned} \tag{4}$$

where m is the circumferential wave number and n is the integer associated with the spherical Bessel functions involved in expressions for the eigenfunctions $U=U_{m,n}$, $V=V_{m,n}$ and $W=W_{m,n}$. Knowing the exact nature of U, V and W is not necessary for this study, but they may be determined using the methods discussed in [2]. The nature of the functions $C(t)=C_{m,n}(t)$ and $S(t)=S_{m,n}(t)$ is still to be determined. In the sequel, for the sake of brevity, we suppress the subscripts m, n if no confusion is likely.

The mathematical formulation given below (in spherical coordinates) is presented within the framework of the three-dimensional theory of linear elasticity and is similar to that presented in [2]. With Lagrange's equations in mind, we formulate expressions for the (approximate) kinetic and potential energies of the vibrating particles in the sphere. The absolute linear velocity of a vibrating particle with its position of rest at point $P(r,\theta,\phi)$ (see Fig. 1) is

$$\mathbf{V}=\frac{\mathrm{d}\mathbf{R}}{\mathrm{d}t}+\boldsymbol{\Omega}\times\mathbf{R}=(\dot w-\varepsilon\Omega v\sin\theta)\hat{\mathbf{r}}+(\dot u-\varepsilon\Omega v\cos\theta)\hat{\boldsymbol{\theta}}+(\dot v+\varepsilon\Omega(u\cos\theta+[r+w]\sin\theta))\hat{\boldsymbol{\phi}}. \tag{5}$$

The kinetic energy of the m,n-vibration mode of a sphere with light mass anisotropy and of radius a is described by

$$E_k=\frac{1}{2}\int_0^{2\pi}\int_0^{\pi}\int_0^{a}\rho(\phi)\ \mathbf{V}\bullet\mathbf{V}\ r^2\sin\theta\,\mathrm{d}r\,\mathrm{d}\theta\,\mathrm{d}\phi. \tag{6}$$

Consequently, neglecting terms of $O(\varepsilon^2)$, Eq. (6) yields

$$E_k=\frac{1}{2}\int_0^{2\pi}\int_0^{\pi}\int_0^{a}\rho(\phi)\{(\dot u^2+\dot v^2+\dot w^2)+2\varepsilon\Omega[(u\dot v-\dot u v)\cos\theta+(\dot v[r+w]-v\dot w)\sin\theta]\}r^2\sin\theta\,\mathrm{d}r\,\mathrm{d}\theta\,\mathrm{d}\phi. \tag{7}$$

Using Eq. (4), notice that

$$\dot u^2=\tfrac{1}{2}U^2[\dot C^2(1+\cos 2m\phi)+\dot S^2(1-\cos 2m\phi)+2\dot C\dot S\sin 2m\phi], \tag{8}$$

with similar expressions for $\dot v^2$,$\dot w^2$,$\dot u v$,$\dot v w$ and $v\dot w$. Now recall, for instance, that (for integers k and m)

$$\int_0^{2\pi}\sin k\phi\sin 2m\phi\,\mathrm{d}\phi=\begin{cases}0 & \text{if } k\neq 2m,\\ \pi & \text{if } k=2m.\end{cases} \tag{9}$$

Hence only the zeroth and $2m$-th harmonics of the Fourier expansion (3) are crucial to the calculation of Eq. (7). Thus the approximate kinetic energy of the m, n-vibration mode of a sphere with light mass anisotropy is

$$E_k=\frac{1}{2}\int_0^{2\pi}\int_0^{\pi}\int_0^{a}\rho_{2m}(\phi)\{(\dot u^2+\dot v^2+\dot w^2)+2\varepsilon\Omega[(u\dot v-\dot u v)\cos\theta+(\dot v[r+w]-v\dot w)\sin\theta]\}r^2\sin\theta\,\mathrm{d}r\,\mathrm{d}\theta\,\mathrm{d}\phi \tag{10}$$

where

$$\rho_{2m}(\phi)=\rho_0[1+\varepsilon(2\Delta_1\cos 2m\phi+2\Delta_2\sin 2m\phi)] \tag{11}$$

and, for the sake of subsequent simplification, we have chosen the Fourier coefficients $a_{2m}=2\Delta_1$ and $b_{2m}=2\Delta_2$. As discussed in [2] with $N=1$ (only one layer is present here), the strain (or potential) energy is given in terms of stresses $\sigma=\sigma_{m,n}$ and strains $\varepsilon=\varepsilon_{m,n}$ by

$$E_p=\frac{1}{2}\int_0^{2\pi}\int_0^{\pi}\int_0^{a}\{\sigma_{rr}\varepsilon_{rr}+\sigma_{\theta\theta}\varepsilon_{\theta\theta}+\sigma_{\phi\phi}\varepsilon_{\phi\phi}+\sigma_{r\theta}\varepsilon_{r\theta}+\sigma_{\theta\phi}\varepsilon_{\theta\phi}+\sigma_{r\phi}\varepsilon_{r\phi}\}r^2\sin\theta\,\mathrm{d}r\,\mathrm{d}\theta\,\mathrm{d}\phi. \tag{12}$$

After substitution of (4) and (11) into (10) and after extensive simplification using computer algebra we determined that

$$E_k(C,S,\dot{C},\dot{S}) = \frac{1}{2}(\dot{C}^2+\dot{S}^2)\pi I_0 + \varepsilon\Omega(\dot{C}S - C\dot{S})\pi I_1 + \left(\frac{\varepsilon\Delta_1}{2}(\dot{C}^2-\dot{S}^2)+\varepsilon\Delta_2\dot{C}\dot{S}\right)\pi I_2, \tag{13}$$

where

$$I_0 = \rho_0\int_0^{\pi}\int_0^{a}[U^2+V^2+W^2]r^2\sin\theta\,\mathrm{d}r\,\mathrm{d}\theta, \tag{14}$$

$$I_1 = 2\rho_0\int_0^{\pi}\int_0^{a}V[U\cos\theta+W\sin\theta]r^2\sin\theta\,\mathrm{d}r\,\mathrm{d}\theta, \tag{15}$$

and

$$I_2 = \rho_0\int_0^{\pi}\int_0^{a}[U^2-V^2+W^2]r^2\sin\theta\,\mathrm{d}r\,\mathrm{d}\theta. \tag{16}$$

As in [2] Eq. (11), the potential energy can be expressed in terms of C and S as

$$E_p(C,S) = \tfrac{1}{2}(C^2+S^2)\pi I_3. \tag{17}$$

For the sake of brevity, the definite integral I_3 is not given explicitly here (unlike the I_j; j=0, 1, 2 above) because the integrand contains many terms involving Young's modulus, Poisson's ratio and the sums of squares and products of eigenfunctions U, V and W, and derivatives $\partial U/\partial r$, $\partial U/\partial\theta$, $\partial V/\partial r$, $\partial V/\partial\theta$, $\partial W/\partial r$ and $\partial W/\partial\theta$. This detail may be readily determined using computer algebra and [2, Eqs. (7) and (8)]. Furthermore, it is not necessary to know the numerical values of the definite integrals I_0,I_1,I_2 and I_3 in this paper. However, these numerical values may be calculated once the eigenfunctions for the m, n-vibration mode are known (see [2]) and they may then be used to calculate constants such as Bryan's factor and the eigenvalue for the m, n-vibration mode (see Eqs. (24)).

3. Bryan's effect for a sphere with light mass imperfections

The Lagrangian of the m, n-vibration mode is given by

$$L(C,S,\dot{C},\dot{S}) = E_k(C,S,\dot{C},\dot{S}) - E_p(C,S). \tag{18}$$

The m, n-vibration mode is governed by the Lagrange–Euler equations of motion

$$\frac{d}{dt}\left(\frac{\partial L}{\partial\dot{C}}\right) - \frac{\partial L}{\partial C} = -\frac{\partial\mathcal{F}}{\partial\dot{C}}, \tag{19}$$

$$\frac{d}{dt}\left(\frac{\partial L}{\partial\dot{S}}\right) - \frac{\partial L}{\partial S} = -\frac{\partial\mathcal{F}}{\partial\dot{S}}, \tag{20}$$

where

$$\mathcal{F} = \frac{\pi D}{2}(\dot{C}^2+\dot{S}^2) \tag{21}$$

is Rayleigh's dissipation function. Let the "isotropic damping factor" be

$$\varepsilon\delta = \frac{D}{2I_0}. \tag{22}$$

We use the symbol ε again to emphasise "smallness", because even though damping is ever present, resonator gyroscopes are manufactured from materials with a high *Quality factor* $Q = 2\pi$ Energy stored/Energy dissipated per cycle.

After substituting (13) and (17) into Eq. (18) and computing the necessary derivatives, Eqs. (19) and (20) yield, respectively, the coupled system of linear ordinary differential equations (ODE) in matrix form:

$$\begin{bmatrix} 1+\varepsilon\Delta_1\xi & \varepsilon\Delta_2\xi \\ \varepsilon\Delta_2\xi & 1-\varepsilon\Delta_1\xi \end{bmatrix}\begin{bmatrix}\ddot{C}\\ \ddot{S}\end{bmatrix} + \omega^2\begin{bmatrix}C\\S\end{bmatrix} = 2\varepsilon\begin{bmatrix}-\eta\Omega\dot{S}-\delta\dot{C}\\ \eta\Omega\dot{C}-\delta\dot{S}\end{bmatrix}, \tag{23}$$

with

$$-1 \le \eta_{m,n} = \frac{I_1}{I_0} \le 1, \quad -1 \le \xi_{m,n} = \frac{I_2}{I_0} \le 1, \quad \omega_{m.n}^2 = \frac{I_3}{I_0}. \tag{24}$$

Note that $\eta_{m,n}$ is Bryan's factor and that $\omega_{m.n}$ is an eigenvalue for the vibrating system as determined in [2] Eqs. (19) and (20) (with N=1) for a perfect spherical body, with or without light isotropic damping. Left multiplying Eq. (23) by the

inverse of the leading coefficient matrix of Eq. (23) and neglecting terms of $O(\varepsilon^2)$, we obtain, to a good approximation:

$$\begin{bmatrix} \ddot{C} \\ \ddot{S} \end{bmatrix} + \omega^2 \begin{bmatrix} 1-\varepsilon\rho_1 & -\varepsilon\rho_2 \\ -\varepsilon\rho_2 & 1+\varepsilon\rho_1 \end{bmatrix} \begin{bmatrix} C \\ S \end{bmatrix} = 2\varepsilon \begin{bmatrix} -\eta\Omega\dot{S}-\delta\dot{C} \\ \eta\Omega\dot{C}-\delta\dot{S} \end{bmatrix}, \tag{25}$$

where we have used the symbols

$$\rho_1 = \Delta_1\xi, \quad \rho_2 = \Delta_2\xi \tag{26}$$

to emphasise the role of the $2m$-th harmonics of the Fourier expansion for density ρ (see Eqs. (3) and (11)). Eq. (25) represents two coupled, simultaneous, linear, ordinary differential equations

$$\ddot{C} + \omega^2 C = \varepsilon f_1(C,S,\dot{C},\dot{S}) \tag{27}$$

and

$$\ddot{S} + \omega^2 S = \varepsilon f_2(C,S,\dot{C},\dot{S}), \tag{28}$$

where

$$f_1 = -2(\eta\Omega\dot{S} + \delta\dot{C}) + (\rho_1 C + \rho_2 S)\omega^2 \tag{29}$$

and

$$f_2 = 2(\eta\Omega\dot{C} - \delta\dot{S}) + (\rho_2 C - \rho_1 S)\omega^2. \tag{30}$$

4. Solutions

For an ideal sphere without damping, which has no inertial rotation ($\varepsilon\Omega = 0$), the right-hand sides of Eqs. (27) and (28) are zero. Reasoning in a manner similar to that discussed in Freidland and Hutton [6], consider parameters $P,Q,m\Theta$ and ψ, which are *constants* that depend on initial conditions. Then it is readily seen via substitution that

$$\begin{aligned} C &= P\cos m\Theta\cos\gamma(t) - Q\sin m\Theta\sin\gamma(t), \\ S &= P\sin m\Theta\cos\gamma(t) + Q\cos m\Theta\sin\gamma(t) \end{aligned} \tag{31}$$

and consequently

$$\begin{aligned} \dot{C} &= -\omega(P\cos m\Theta\sin\gamma(t) + Q\sin m\Theta\cos\gamma(t)), \\ \dot{S} &= -\omega(P\sin m\Theta\sin\gamma(t) - Q\cos m\Theta\cos\gamma(t)), \end{aligned} \tag{32}$$

with

$$\gamma(t) = \omega t + \psi \tag{33}$$

yield a periodic solution to the system of ODE (27) and (28). Thus the orbit of the point (C,S) in the CS-plane is an ellipse with P and Q the lengths of the major and minor semi-axes, respectively, $m\Theta$ the angle between the C-axis and the major axis of the ellipse and ψ a phase angle.

For a perfectly manufactured sphere, if the inertial angular rate $\varepsilon\Omega$ is nonzero and light isotropic damping is present, then Eq. (30) of [2] indicates that the orbit will appear to be a slowly shrinking ellipse which is slowly precessing with a precession rate of $\eta\varepsilon\Omega$ where η is Bryan's factor (see Eq. (24)). This precession was also noted by [6] in the absence of damping. Consequently, some or all of the quantities P,Q,Θ and ψ are slowly varying, unlike C or S, which are rapidly varying. As observed by [6] just after Eq. (2.10), the rapidly varying quantities C and S are "difficult to relate to the" inertial angular rate, while the behaviour of the slowly varying quantities P,Q,Θ and ψ "may be expected to be more indicative of the" inertial angular rate. Consequently we generalise the method of [6] and Lynch [5] by introducing a change from "fast" to "slow" variables $(C(t),S(t),\dot{C}(t),\dot{S}(t)) \longrightarrow (P(t),Q(t),\Theta(t),\psi(t))$. This is achieved by considering the transformation:

$$C(t)\cos m\phi + S(t)\sin m\phi = P(t)\cos m(\phi-\Theta(t))\cos(\omega t+\psi(t)) + Q(t)\sin m(\phi-\Theta(t))\sin(\omega t+\psi(t)). \tag{34}$$

Without loss of generality assume that $P \neq 0$. If $Q=0$, the right-hand side of Eq. (34) represents a standing wave, whereas if $0 \neq P = Q$, it represents a travelling wave. If $0 \neq P \neq Q \neq 0$, then it represents a phenomenon which is a "mixture" between a standing and travelling wave which we call a *precessing wave*. This name is appropriate because, even if the inertial rotation rate $\varepsilon\Omega$ is zero, the vibration pattern undergoes slow precession owing to the presence of the light mass anisotropy, as we demonstrate below.

Without loss of generality, assume that $0 \neq P \neq Q$. Proceeding from Eq. (34), using double-angle identities, we find that

$$C\cos m\phi + S\sin m\phi = \cos m\phi[P\cos m\Theta\cos(\omega t+\psi) - Q\sin m\Theta\sin(\omega t+\psi)] + \sin m\phi[P\sin m\Theta\cos(\omega t+\psi) + Q\cos m\Theta\sin(\omega t+\psi)]. \tag{35}$$

By equating the coefficients of $\cos m\phi$ and $\sin m\phi$ on both sides of Eq. (35), it follows that the transformation requires that

$$C(t) = P(t)\cos m\Theta(t)\cos\gamma(t) - Q(t)\sin m\Theta(t)\sin\gamma(t),$$

$$S(t) = P(t)\sin m\Theta(t)\cos\gamma(t) + Q(t)\cos m\Theta(t)\sin\gamma(t), \tag{36}$$

with

$$\gamma(t) = \omega t + \psi(t). \tag{37}$$

To interpret this transformation, regard $C(t)$ as the "cosine" and $S(t)$ as the "sine" output of a vibratory gyroscope connected to a two-channel oscilloscope. Then the Lissajous figure produced on the oscilloscope screen will resemble the slowly shrinking, slowly precessing ellipse-like orbit which we call a *precessing-ellipse*, depicted in Fig. 2, where

- the major semi-axis of the precessing-ellipse $P(t)$ represents the amplitude of the *principal* or *in-phase* precessing wave;
- the minor semi-axis of the precessing-ellipse $Q(t)$ represents the amplitude of the *quadrature* precessing wave;
- $m\Theta(t)$ is the angle between the C-axis and the major axis of the precessing-ellipse; and
- $\psi(t)$ is the *phase angle* of the vibrating pattern.

The angle $m\Theta$ is called the *precession* (or *electrical*) angle of the vibrating pattern and the quantity $\sqrt{P^2+Q^2}$ is the amplitude of the vibrating pattern. Hence $m\dot{\Theta}$ is the rate of rotation of the vibrating pattern within the rotating reference frame $Oxyz$ and is called the *precession rate*. According to [6], on page 546, the *orbital angle* $\gamma(t) = \omega t + \psi(t)$ indicated here in Fig. 2 is the angle on a circle, with centre at (0,0) of radius P measured anti-clockwise from the major axis to a line through a point A which is at the intersection of the circle and a line parallel to the minor axis through the point (C,S). The point A has no physical significance but has the property that it moves with an angular rate ω.

Keeping in mind that $\dot{\gamma} = \omega + \dot{\psi}$ and examining the expression for $\dot{C}$ and $\dot{S}$, assume, respectively, that

$$\dot{P}\cos m\Theta\cos\gamma - \dot{Q}\sin m\Theta\sin\gamma - m\dot{\Theta}[P\sin m\Theta\cos\gamma + Q\cos m\Theta\sin\gamma] - \dot{\psi}[P\cos m\Theta\sin\gamma + Q\sin m\Theta\cos\gamma] = 0 \tag{38}$$

and

$$\dot{P}\sin m\Theta\cos\gamma + \dot{Q}\cos m\Theta\sin\gamma + m\dot{\Theta}[P\cos m\Theta\cos\gamma - Q\sin m\Theta\sin\gamma] - \dot{\psi}[P\sin m\Theta\sin\gamma - Q\cos m\Theta\cos\gamma] = 0. \tag{39}$$

This yields, respectively:

$$\dot{C}(t) = -\omega[P(t)\cos m\Theta(t)\sin\gamma(t) + Q(t)\sin m\Theta(t)\cos\gamma(t)],$$

$$\dot{S}(t) = -\omega[P(t)\sin m\Theta(t)\sin\gamma(t) - Q(t)\cos m\Theta(t)\cos\gamma(t)]. \tag{40}$$

Thus with (36) and (40) we have achieved what [6] discussed on page 546 for the case $m=1$. From Eq. (40), by differentiation, and because

$$\omega\dot{\gamma} = \omega^2 + \omega\dot{\psi}, \tag{41}$$

it follows that

$$\ddot{C} + \omega^2 C = -\omega F_1(\dot{P},\dot{Q},m\dot{\Theta},\dot{\psi},P,Q,m\Theta,\psi) \tag{42}$$

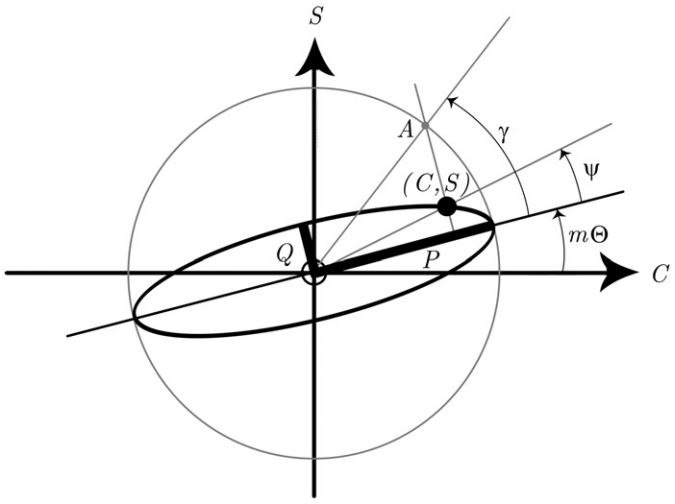

Fig. 2. Lissajous figure on the screen of a two-channel oscilloscope representing a "precessing-ellipse".

and

$$\ddot{S}+\omega^2 S=-\omega F_2(\dot{P},\dot{Q},m\dot{\Theta},\dot{\psi},P,Q,m\Theta,\psi), \tag{43}$$

where

$$F_1=\dot{P}\cos m\Theta\sin\gamma+\dot{Q}\sin m\Theta\cos\gamma-m\dot{\Theta}[P\sin m\Theta\sin\gamma-Q\cos m\Theta\cos\gamma]+\dot{\psi}[P\cos m\Theta\cos\gamma-Q\sin m\Theta\sin\gamma] \tag{44}$$

and

$$F_2=\dot{P}\sin m\Theta\sin\gamma-\dot{Q}\cos m\Theta\cos\gamma+\dot{m}\Theta[P\cos m\Theta\sin\gamma+Q\sin m\Theta\cos\gamma]+\dot{\psi}[P\sin m\Theta\cos\gamma+Q\cos m\Theta\sin\gamma]. \tag{45}$$

Substituting Eqs. (36) and (40) into Eqs. (29) and (30) yields f_1 and f_2 in terms of the transformed variables, that is, $f_1=f_1(P,Q,m\Theta,\gamma)$ and $f_2=f_2(P,Q,m\Theta,\gamma)$. We now have a system of four equations with four unknowns, namely Eqs. (38) and (39) together with

$$F_1(\dot{P},\dot{Q},m\dot{\Theta},\dot{\psi},P,Q,m\Theta,\psi)=-\frac{\varepsilon}{\omega}\,f_1(P,Q,m\Theta,\gamma) \tag{46}$$

and

$$F_2(\dot{P},\dot{Q},m\dot{\Theta},\dot{\psi},P,Q,m\Theta,\psi)=-\frac{\varepsilon}{\omega}\,f_2(P,Q,m\Theta,\gamma), \tag{47}$$

where Eq. (46) (respectively, Eq. (47)) is obtained by comparing the right-hand sides of Eqs. (27) and (42)) (respectively, Eqs. (28) and (43)). These four equations may be written in terms of a coefficient matrix **M** as follows:

$$\mathbf{M}\begin{bmatrix}\dot{P}\\ \dot{Q}\\ m\dot{\Theta}\\ \dot{\psi}\end{bmatrix}=\begin{bmatrix}0\\ 0\\ -\frac{\varepsilon}{\omega}f_1(P,Q,m\Theta,\gamma)\\ -\frac{\varepsilon}{\omega}f_2(P,Q,m\Theta,\gamma)\end{bmatrix}. \tag{48}$$

Multiplication of Eq. (48) from the left by $\mathbf{M}^{-1}$ yields the coupled system of nonlinear first-order ODEs (with "slow variables" P,Q,Θ and ψ and "fast variable" γ):

$$\dot{P}=-\frac{\varepsilon}{\omega}[f_1\cos m\Theta+f_2\sin m\Theta]\sin\gamma,$$

$$\dot{Q}=-\frac{\varepsilon}{\omega}[f_1\sin m\Theta-f_2\cos m\Theta]\cos\gamma,$$

$$m\dot{\Theta}=\frac{\varepsilon}{\omega(P^2-Q^2)}\{[P\sin m\Theta\sin\gamma+Q\cos m\Theta\cos\gamma]f_1-[P\cos m\Theta\sin\gamma-Q\sin m\Theta\cos\gamma]f_2\},$$

$$\dot{\psi}=-\frac{\varepsilon}{\omega(P^2-Q^2)}\{[P\cos m\Theta\cos\gamma+Q\sin m\Theta\sin\gamma]f_1+[P\sin m\Theta\cos\gamma-Q\cos m\Theta\sin\gamma]f_2\}. \tag{49}$$

In order to better understand the system of ODE (49), consider the averaging operator

$$\langle-\rangle=\frac{1}{2\pi}\int_0^{2\pi}(-)\,d\gamma, \tag{50}$$

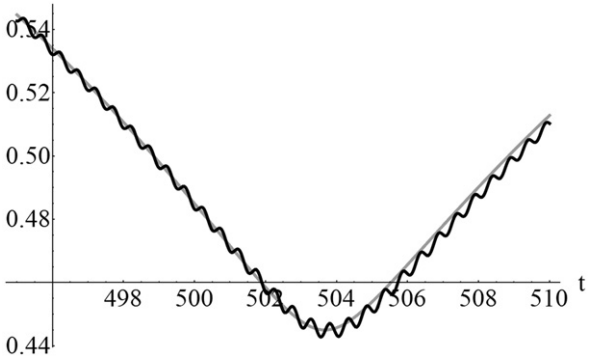

Fig. 3. There is close agreement between the nonaveraged principal vibration P (the black curve) and the averaged quantity (the grey curve).

with regard to the fast variable γ. We used computer algebra (otherwise the calculations are tedious) to verify that the averages of the functions in Eqs. (49) are given by

$$\dot{P} = \frac{\varepsilon\omega}{2} Q[\rho_1 \sin 2m\Theta - \rho_2 \cos 2m\Theta] - \varepsilon\delta P,$$

$$\dot{Q} = -\frac{\varepsilon\omega}{2} P[\rho_1 \sin 2m\Theta - \rho_2 \cos 2m\Theta] - \varepsilon\delta Q,$$

$$m\dot{\Theta} = \eta\varepsilon\Omega + \varepsilon\omega \frac{PQ}{(P^2 - Q^2)}[\rho_1 \cos 2m\Theta + \rho_2 \sin 2m\Theta],$$

$$\dot{\psi} = -\frac{\varepsilon\omega}{2} \frac{(P^2 + Q^2)}{(P^2 - Q^2)}[\rho_1 \cos 2m\Theta + \rho_2 \sin 2m\Theta]. \tag{51}$$

Except for the phase shift, when we solved and visualised both the "nonaveraged" system of ODEs (49) and the "averaged" system of ODEs (51) by means of computer algebra, it was evident that the respective solutions agree closely but are not identical. The "nonaveraged" and "averaged" phase shifts initially agree and, with evolution in time, show similar trends.

From the system of ODEs (51) it appears that the inertial angular rate $\varepsilon\Omega$ does not influence changes with time in the amplitudes P and Q or the phase ψ. The light mass imperfection causes changes with time which appear to be of a damped vibratory nature for both the quadrature component Q as well as the principal component P, as indicated in Fig. 4. The precession angular rate $m\dot{\Theta}$ appears to depend on the inertial angular rate as well as the quadrature component Q of the vibration, but is not influenced by the damping factor δ. It is not directly proportional to the inertial angular rate $\varepsilon\Omega$ as is the case for a perfect isotropically damped structure where the constant of proportionality is Bryan's factor η. If the quadrature component is not suppressed, then a "capture effect" (as indicated in Fig. 5) appears to occur, namely that the precession angle $m\Theta$ will not grow at a constant rate but shows periodic behaviour. It appears that the damping factor does not influence changes with time in the phase shift ψ and that the light mass imperfection substantially influences these changes. The phase shift appears to be negative, strictly decreasing and unbounded.

5. Example

The following numerical experiment considers the influence of light mass imperfection and light isotropic damping in a slowly rotating ball with regard to the dynamics of its vibrating pattern. We solve systems (49) and (51) using the

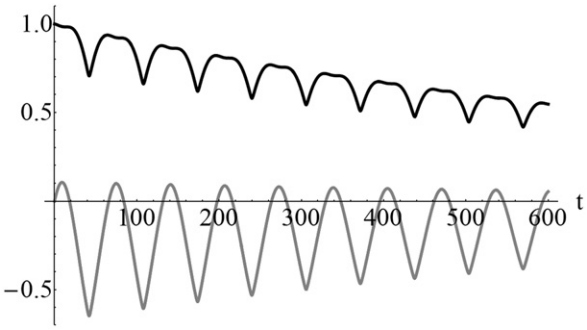

Fig. 4. The black curve represents damped principal vibration (P) while the grey curve represents damped quadrature vibration (Q).

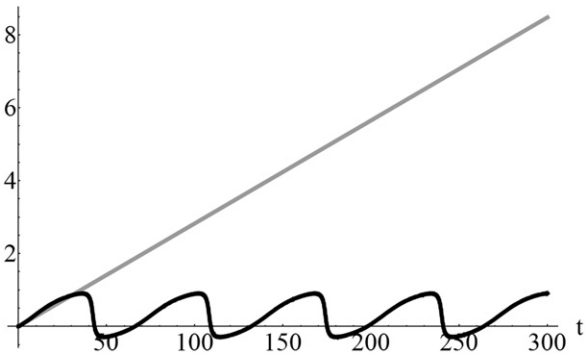

Fig. 5. The precession angle $m\Theta$ for a slowly rotating vibrating sphere with light mass imperfections is "captured" periodically (the black curve) while the ideal case precession angle $\eta\varepsilon\Omega t$ increases linearly (the grey line).

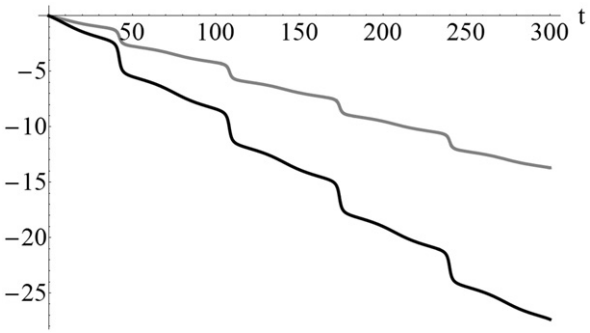

Fig. 6. The averaged phase angle ψ (grey curve) and nonaveraged phase angle ψ (black curve) agree initially and show similar trends with evolution in time.

"NDSolve" routine of *Mathematica*® set at default "WorkingPrecision". We have checked that default precision yields at least 5 digits of accuracy over the interval $0 \le t \le 600$ s using methods similar to those described in [7]. For this example, let $\varepsilon = \frac{1}{100}, \omega = 2\pi \text{ rad s}^{-1}, \eta = \frac{9}{10}, \Omega = \pi \text{rad s}^{-1}, \rho_1 = 1, \rho_2 = \frac{7}{10}, m = 2$ and $\delta = \frac{1}{10}$ s^{-1} and choose initial conditions as $P(0)=1$, $Q(0)=0$, $\Theta(0) = 0$ rad and $\psi(0) = 0$ rad. Visual inspection of the eight solutions shows that an averaged quantity exhibits the same trend as the corresponding nonaveraged quantity with evolution in time. This trend is close for P, Q and $m\Theta$. For instance, this can be seen clearly in Fig. 3 for P. The damped behaviour of the principal and quadrature vibrations is evident when one observes P and Q in Fig. 4.

For small inertial angular rates $\varepsilon\Omega$, Fig. 5 demonstrates the "capture effect" in comparison with the pattern's precession in an ideal state (where no light mass (or other) imperfections are present), with or without isotropic viscous damping. The thick grey line indicates the ideal case with the precession angle $m\Theta = \eta\varepsilon\Omega t$ changing linearly, while the light mass imperfection-induced precession angle $m\Theta$ initially shows a linear tendency but is then "captured" in what appears to be a periodic manner.

The averaged and nonaveraged phase angles ψ agree initially and then show a similar trend with evolution in time as demonstrated by Fig. 6.

6. Conclusions

In order to study the effects of light mass imperfections on slowly rotating vibrating bodies, we introduced a new system of variables. This allowed us, using inter alia, the method of averaging, to predict, how principle and quadrature vibrating patterns will change with time. We demonstrated that an apparent "capture effect" occurs with the precession angle and that phase shift appears to be negative, strictly decreasing and unbounded. We demonstrated that if light isotropic damping is taken into account, then damped vibratory motion appears to take place but the damping does not affect the precession angle or phase shift.

We have developed mathematical tools which will facilitate future study which we have earmarked to include anisotropic damping, prestress, nonlinear elasticity and methods to control their effects in a resonator gyroscope.

Acknowledgements

This material is based upon work supported financially by the Tshwane University of Technology (TUT), the Council for Scientific and Industrial Research (CSIR) of South Africa and the National Research Foundation (NRF) of South Africa (NRF grant reference number ICD 2006 0711 0000 6). Any opinions, findings and conclusions or recommendations expressed in this material are those of the authors and therefore the TUT, the CSIR and the NRF do not accept any liability in regard thereto.

References

[1] G.H. Bryan, On the beats in the vibrations of a revolving cylinder or bell, *Proceedings of the Cambridge Philosophical Society* 7 (1890) 101–111.
[2] M.Y. Shatalov, S.V. Joubert, C.E. Coetzee, I. Fedotov, Free vibration of rotating hollow spheres containing acoustic media, Available online: doi: 10.1016/j.jsv.2008.11.020, accessed April 2009, *Journal of Sound and Vibration* 322 (4–5) (2009) 1038–1047.
[3] V. Zhuravlev, D. Klimov, *Applied methods in the theory of oscillations*, Nauka, Moscow, 1988 (in Russian).
[4] E.J. Loper Jr., D.D. Lynch, Hemispherical resonator gyroscope, U.S. Patent No. 4,951,508, 1990.
[5] D.D. Lynch, Vibratory gyro analysis by the method of averaging, *Proceedings of the Second Saint Petersburg International Conference on Integrated Navigation Systems* (1995) 26–34.
[6] B. Friedland, M.F. Hutton, Theory and error analysis of vibrating member gyroscope, *IEEE Transactions on Automatic Control* AC-23 (4) (1978) 545–556.
[7] S.V. Joubert, J.C. Greeff, Accuracy estimates for computer algebra system IVP solvers, *South African Journal of Science* 102 (2006) 46–50.